EXPERIMENTAL APPROACH TO ASSESS EVAPORATIVE COOLING UNDER FORCED AIR FLOW

L. G. G. Rodrigues, E. I. B. Parisotto, B. A. M. Carciofi[*] and J. B. Laurindo

Department of Chemical and Food Engineering, Federal University of Santa Catarina,
EQA/CTC/UFSC, CEP: 88040-900, Florianópolis - SC, Brazil.
Phone.: +55 48 37215229; Fax: +55 48 37219687.
E-mail: bruno.carciofi@ufsc.br

Abstract - Air blast is one of the most employed industrial chilling methods. It can be enhanced, i.e., increasing heat transfer and reducing cooling time, by superficial evaporative phenomena. This work reports a methodology, including experimental setup and mathematical modelling, to quantify the air chilling enhancement by wetting the surface of the object to be chilled. A spherical metal model was covered by a cotton tissue (wet or dry) and placed into a cold chamber. The effective heat transfer coefficient was determined at different temperature, air velocity, and relative humidity from time-temperature profiles into the sphere. Under the same air conditions, the effective coefficient between sphere and air was increased three-fold by moistening the cotton tissue on the sphere surface. Furthermore, comparing a dry and wet surface showed that evaporative cooling resulted in much shorter chilling times. The proposed approach was able to assess evaporative heat transfer by measuring only the time-temperature profile, and is suitable for industrial applications.
Keywords: Air blast chilling; Cold chamber; Convection; Heat and mass transfer; Effective heat transfer coefficient.

INTRODUCTION

Chilling processes are very important in many industries, such as in the food industry, in order to inhibit microbial growth and preserve the quality of foodstuffs from the producer to the consumer. Air blast chilling of foods can involve both heat transfer between the product and the chilling medium and mass transfer due to water evaporation (weight loss) at the wet surface (Mekprayoon and Tangduangdee, 2012). Processing time and weight loss are important parameters regarding the design of chilling lines for the quality of many food products. Conventional methods such as slow air, air blast, water immersion, and water spraying have been widely used in in-

dustrial chilling of food products (Dincer, 1997a; Sun and Wang, 2004; Laurindo *et al*., 2010a; Laurindo *et al*., 2010b), each one with its own advantages and disadvantages. Alternatively, rapid chilling methods increase food safety, improve quality, prevent microbial growth, and might reduce evaporative weight losses (Erdogdu *et al*., 2005).

It is well known that water chilling is a very efficient procedure for food cooling due to the high heat transfer coefficients between the product and chilling water (Laurindo *et al*., 2010b). Some products such as peas, radishes, cantaloupes, peaches, cherries, oranges, shrimps, crabs, sardines, tuna, and poultry carcasses are usually cooled by water immersion (Dincer, 1997b; Lucas and Raoult-Wack, 1998; Teruel

---

*To whom correspondence should be addressed

et al., 2003; Amendola and Teruel, 2005). In the poultry industry, carcasses are traditionally cooled from approximately 40 °C to 4 °C by immersion in cold water (or a mixture of ice and water), which is crucial to ensure safe products (James *et al.*, 2006; Carciofi and Laurindo, 2007; Carciofi and Laurindo, 2010). On the other hand, air chilling is gaining in popularity because of the limited availability of water, wastewater discharge restrictions, and governmental regulations on carcass moisture retention (Huezo *et al.*, 2007). Evaporative air chilling, a mixed type of air chilling and water chilling, combine the advantages of both methods and is an alternative to immersion chilling of poultry carcasses (Mielnik *et al.*, 1999, Jeong *et al.*, 2011). In a typical cold-air meat chilling process, the water vapor pressure at the meat surface is much higher than in the cooling air, resulting in water evaporation (weight and quality losses). Consequently, water from inside diffuses towards the surface as a result of moisture gradients, and the balance between evaporation and diffusion governs the water activity near the surface. The intensity of these coupled phenomena determines the chilling time, weight loss, temperature, and surface water activity (Trujillo and Pham, 2006). Chuntranuluck *et al.* (1998) developed a model for predicting chilling times of foods when evaporative chilling is significant. They used finite difference analysis to simulate transient chilling of food products of simple shapes such as spheres, infinite slabs, and cylinders. Those authors showed how to account for evaporative chilling considering the latent heat of evaporation and the evaporative weight loss rate.

The most significant factors for the design of a refrigerated food chain are the food's thermophysical properties (e.g., specific heat, thermal conductivity, thermal diffusivity) and the chilling heat transfer parameters (heat transfer coefficients) (Dincer, 1997b). The convective heat transfer coefficient is a key parameter to calculate chilling time, and, hence, in the design of food-cooling facilities (hydro-chilling, air chilling) (Cuesta *et al.*, 2012). This coefficient is a local or global parameter, which depends mainly on the velocity of the surrounding fluid, product geometry, flow orientation, surface roughness, and on the packaging (Incropera and Dewitt, 2002; Becker and Fricke, 2004). At high heat transfer rates, food shape will play a minor role. The effect of these various factors on convection heat transfer can be mathematically expressed as a relationship of dimensionless numbers: Nusselt (*Nu*), Reynolds (*Re*), Prandtl (*Pr*), and Grashof (*Gr*) (Incropera and Dewitt, 2002; Verboven *et al.*, 2003).

Landfeld and Houska (2006) used a metallic chicken as a simplified physical model to estimate the convective heat transfer coefficient in an air blast chilling tunnel. They reported coefficient values between the metallic model and the chilling media close to 50 W m^{-2} K^{-1}. Verboven *et al.* (2003) reported results of convective heat transfer coefficients between stationary spherical particles and an aqueous solution inside a hydrofluidized freezing unit ranging from 154 to 1548 W $m^{-2}K^{-1}$. These values depended on the body diameter, chilling fluid temperature, and fluid agitation level. The authors attributed the variability of the measured coefficients to non-constant flow and turbulence fields in the aqueous medium.

The lack of actual data about the effect of cooling conditions on the chilling rates, weight loss, and quality is a major barrier to the advancement of technology related to this unit operation (James *et al.*, 2006). In this study, the objective was to assess the heat transfer between the cooling air and a metallic sphere, chosen as a model, covered by a wet or dry cotton tissue and to propose a methodology to obtain an effective heat transfer coefficient taking into account mass transfer phenomena, but without measuring it. The enhancement of this effective coefficient and the cooling rates provided by wetting the surface were evaluated from the experimental temperature analysis.

MATERIALS AND METHODS

In order to evaluate the contribution of evaporative cooling on the heat transfer between a metallic sphere and air, effective heat transfer coefficients were determined from three different arrangements: i) uncovered aluminum sphere, ii) aluminum sphere covered with a dry cotton tissue, and iii) aluminum sphere covered with a wet cotton tissue. The purpose-built experimental setup, the instruments used to determine the experimental conditions, and the mathematical and statistical approaches are described below.

Experimental Setup

The experimental setup used in this study consists of a cold chamber (0.95 m x 1.02 m x 0.98 m) equipped with a temperature and relative humidity (RH) control system. For controlling the air temperature inside the cold chamber, a PID controller (NOVUS, model N1100, Porto Alegre, Brazil) acting on an electrical heating element placed inside the cooling chamber was used. Pre-defined temperatures and RH inside the chamber were achieved by controlling the electric

heating element, while the compressor capacity was controlled using a frequency inverter (Danfoss, model VLT Micro Drive FC 51, Beijing, China) (Danfoss, model 136 LCZ, Osasco, Brazil). The Field Chart software (Novus, version 1.8, Porto Alegre, Brazil) registered temperature and RH data inside the chamber. Airflow patterns inside the chamber were provided by a fan (WEG, 1000 rpm, Jaraguá do Sul, Brazil) at two average air velocities: 0.92 m s^{-1} (V_1) and 1.42 m s^{-1} (V_2). These average air velocities over the sphere were measured by a digital anemometer (Testo 425, Lenzkirch, Germany) positioned 0.50 m from the fan, as shown in Figure 1.
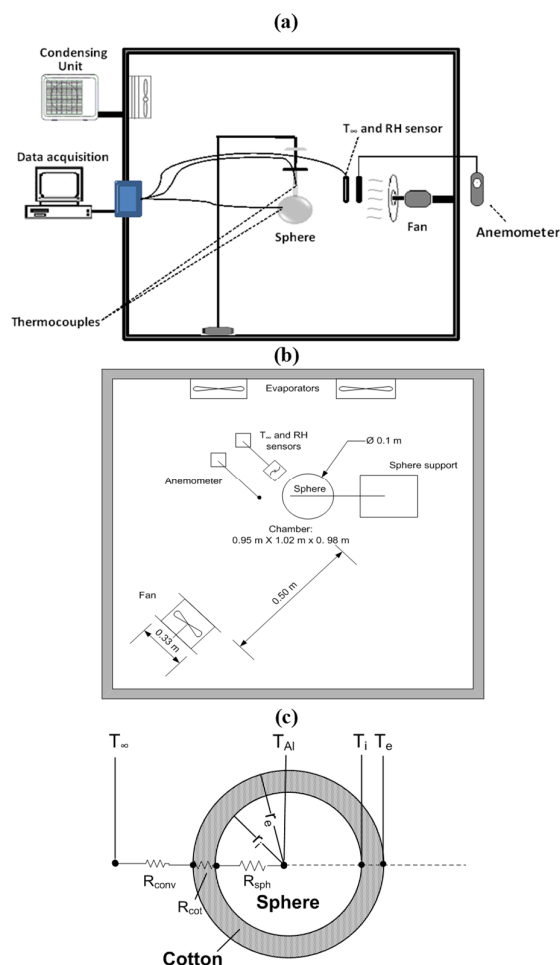
Figure 1: (a) Schematics of the forced-air chilling process of a sphere. (b) Plan view of the forced-air chilling process of a sphere. (c) Schematics of the sphere covered with cotton, sensor positions, and thermal resistance network: convective (R_{conv}), conductive in the cotton (R_{cot}), and conductive in the sphere (R_{sph}).

An aluminum sphere (diameter, $D_{Al} = 0.100$ m, and mass, $m_{Al} = 1.41$ kg) was used as a model to

assess the influence of the surface condition (dry or wet) on heat transfer. For that, convective heat transfer coefficient values between the sphere and the cooling air were determined under different conditions: both velocities (V_1 and V_2) at three RH conditions (30%, 60%, and 90%). Aluminum's physical properties were density, $\rho_{Al} = 2702$ kg m^{-3}; specific heat, $c_{Al} = 903$ J kg^{-1} K^{-1}; and thermal conductivity, $k_{Al} = 237$ W m^{-1} K^{-1} (Incropera and Dewitt, 2002). A rigid polyethylene rod was used in order to support the sphere during the cooling experiments; this polymer was chosen to prevent the effects of conduction heat transfer through itself.

The sphere's core temperature (T_{Al}) was measured using a T-type thermocouple (IOPE, model 24 AWG, São Paulo, Brazil) inserted into the sphere's geometric center through a channel made with a precision mechanical machine. The channel was filled with thermal paste (IPT300, Implastec, São Paulo, Brazil) and sealed with a commercial epoxy resin (Professional Araldite, Brascola, São Paulo, Brazil). Time-temperature data of cooling air (T_∞) were measured, as well as time-temperature data of internal (T_i, in contact with the aluminum sphere's surface) and external (T_e, in contact with air) cotton tissue surfaces. The dry cotton tissue mass (m_d) was 0.009 kg, while its specific heat was 1300 J kg^{-1} K^{-1} (Incropera and Dewitt, 2002). The diameter of the sphere covered with cotton tissue was $D_e = 0.102$ m. Figure 1c is a schematic that represents the sphere covered with cotton, the sensor positioning, and the three resistances to heat transfer present in the forced air chilling process. Contact resistances between cotton and aluminum were neglected. R_{conv}, R_{cot}, and R_{sph} denote convective thermal resistances (between air and surface), conductive thermal resistances in the cotton, and conductive thermal resistances in the aluminum.

All temperatures were monitored with T-type thermocouples (IOPE, model A-TX-TF-TF-R 30 AWG, São Paulo, Brazil) and recorded at 5 s intervals by a data acquisition system (Agilent, model 34972A, Santa Clara, USA).

Determination of Heat Transfer Coefficients Between the Sphere and Forced Air

Aluminum Sphere

Initially, the aluminum sphere was heated in a thermoregulated bath (Tecnal, model TE - 184, Piracicaba, Brazil) up to 38-39 °C and kept in water to reach a spatially homogeneous temperature. Next, the sphere was quickly introduced into the cold

chamber. The cooling process was monitored until the sphere's core temperature had reached 4.0 °C. This procedure was done in quintuplicate for cooling air at each predetermined air velocity and at 1.0 °C.

The convective heat transfer coefficient (h) between the sphere and air was determined from experimental time-temperature evolutions at both the sphere's core and air chilling using the well-known lumped capacitance method. This method can be used when the thermal resistance to heat transfer by conduction within one solid is much smaller than the thermal resistance to heat transfer between the solid's surface and fluid flow. In other words, the lumped capacitance method can be applied only when the temperature inside the solid can be considered spatially uniform at any given time during the process, i.e., it is practical only if the Biot number (Eq. (1)) is less than 0.1 (Incropera and Dewitt, 2002).

$$Bi = \frac{Lh}{k_{Al}} \qquad (1)$$

in which L is the solid's characteristic dimension, defined as the ratio between its volume and interfacial area. For a sphere, $L = D_{Al}/6$. This way, if $Bi < 0.1$, the global energy balance in the whole solid is given by Eq. (2).

$$-hA_{Al}(T_{Al} - T_\infty) = m_{Al}c_{Al}\frac{dT_{Al}}{dt} \qquad (2)$$

in which A_{Al} is the interfacial area of the aluminum sphere and t is the cooling time.

Integrating Eq. (2) leads to Eq. (3), from which the h value can be determined using experimental time-temperature data.

$$\ln\left[\frac{(T_o - T_\infty)}{(T_{Al} - T_\infty)}\right] = \frac{hA_{Al}}{m_{Al}c_{Al}}(t - t_o) \qquad (3)$$

in which T_o is the solid's temperature at initial time t_o (initial condition).

Aluminum Sphere Covered with Cotton Tissue

An effective convective heat transfer coefficient (h_{ef}), which has both thermal and evaporative contribution, was determined from time-temperature data and Eq. (4), which represents the overall energy balance in the aluminum sphere covered with the cotton tissue,

$$-h_{ef}A_e(T_e - T_\infty) = m_c c_c \frac{d\overline{T_c}}{dt} + m_{Al}c_{Al}\frac{dT_{Al}}{dt} \qquad (4)$$

in which A_e is the surface area of the aluminum sphere covered by the wet cotton tissue; and m_c and c_c are the mass and the specific heat of the wet cotton, respectively.

Assuming the temperature inside the aluminum sphere as spatially uniform at any given time during the process and a pseudo-stationary approach, Eq. (5) allows calculating an average temperature ($\overline{T_c}$) in the cotton spherical shell ($r_i \leq r \leq r_e$, from the aluminum sphere's surface, radius r_i, and cotton surface, radius r_e),

$$\overline{T_c} = \frac{\int_{r_i}^{r_e} T_c(r)4\pi r^2 dr}{\int_{r_i}^{r_e} 4\pi r^2 dr} \qquad (5)$$

in which $T_c(r)$ represents the temperature in the spherical shell, as given by Eq. (6) for a steady state (Incropera and Dewitt, 2002).

$$T_c(r) = T_i - (T_i - T_e)\left(\frac{1 - \dfrac{r_i}{r}}{1 - \dfrac{r_i}{r_e}}\right) \qquad (6)$$

Thus, after integration, $\overline{T_c}$ is given by Eq. (7).

$$\overline{T_c} = T_i - \frac{(T_e - T_i)\left(r_e^4 - \dfrac{3}{2}r_e^3 r_i + \dfrac{1}{2}r_e r_i^3\right)}{\left(r_e^3 - r_i^3\right)(r_e - r_i)} \qquad (7)$$

Mass and specific heat were assumed to be constant for the aluminum sphere and variable for the wet cotton as a consequence of moisture content in the tissue. Time-dependence was calculated from the cotton tissue's moisture content, as given by Eq. (8),

$$m_c c_c = m_d c_d + m_w c_w \qquad (8)$$

in which $m_d c_d$ and $m_w c_w$ are the product between mass and specific heat of dry cotton around the aluminum sphere and water soaked into the tissue, respectively. Specific heat of cotton and water were assumed as 1300 J kg^{-1} K^{-1} and 4180 J kg^{-1} K^{-1}, respectively (Incropera and Dewitt, 2002).

The dry cotton tissue's mass (m_d) was constant at 0.009 kg, while water mass decreased during the evaporative cooling. In order to evaluate m_w as a function of time, the wet cotton tissue was weighed outside the chamber on a semi-analytical balance (Gehaka, model BG 400, São Paulo, Brazil). At pre-determined intervals, the sphere was quickly re-moved from the chamber and placed on the balance. The result was expressed as a percentage of the water present in the cotton tissue. The initial mass was determined from ten measurements (average value = 0.0338 kg and standard deviation = 0.0003 kg). Time-water mass data were fitted by the empirical Eq. (9),

$$m_w = a \exp(-bt) + c \qquad (9)$$

in which a, b and c are empirical constants.

One instantaneous coefficient value was calculated from each recorded time interval (Δt) using Eq. (4) re-written as Eq. (10). Thus, one average coefficient was determined from each cooling assay. Finally, the average value of h_{ef} is the average from five cooling assays at each experimental setup investigated.

$$h_{ef} = \frac{1}{A_e(T_e - T_\infty)}\left(m_c c_c \frac{\Delta \overline{T_c}}{\Delta t} + m_{Al} c_{Al} \frac{\Delta T_{Al}}{\Delta t} \right) \qquad (10)$$

in which T_e, T_∞, m_c, c_c, $\Delta \overline{T_c}$, and ΔT_{Al} were the experimental results recorded at each $\Delta t = 5$ s.

The h_{ef} values when the sphere was covered by the dry cotton tissue were determined as a particular case in which m_w was constant and equal to zero.

Correlation for Air-Sphere Convective Heat Transfer Coefficient

Some well-known empirical correlations can be used to estimate the convective heat transfer coefficient between a solid sphere and a fluid without simultaneous mass transfer. McAdams proposed an empirical correlation to estimate the convection heat transfer coefficient between a sphere and a gas (Eq. (11)) in which all properties are evaluated at the film's temperature. This correlation is limited to $17 < Re < 70,000$ (McAdams, 1954; Holman, 1992),

$$Nu = \frac{hD}{k_\infty} = 0{,}37(\mathrm{Re})^{0,6} = 0{,}37\left(\frac{\rho_\infty D}{v}\right) \qquad (11)$$

in which Nu is the Nusselt Number; D is the sphere's diameter (D_{Al} or D_e); and k_∞, ρ_∞, and v are the gas's (air) thermal conductivity, density, and kinematic viscosity, respectively. In the present study, Re

values were close to 7,000 and 10,500 at V_1 and V_2, respectively.

Statistical Analysis

Estimated parameters were evaluated by one-way ANOVA at 95% probability level. In cases with significant effects ($p < 0.05$), the average values were compared using Tukey's test.

RESULTS AND DISCUSSION

Convective Heat Transfer Coefficients

Table 1 summarizes h and h_{ef} values determined from experimental time-temperature data and those estimated from McAdams correlation. It is remarkable that, in all experimental conditions, Bi values were equal to or less than 10^{-2}, indicating that there were no significant temperature gradients inside the metallic sphere and that the lumped method was properly chosen. Estimated values of h and h_{ef} had low coefficients of variation ($CV < 10\%$), indicating reproducibility. The coefficient of determination (R^2) of the linear regression (Eq. (3)) to experimental data ranged from 0.987 to 0.999.

In the present study, both predicted (McAdams correlation) and experimental coefficients are of the same order of magnitude. Predicted h values between the uncovered sphere and air flowing around it were 23.0% and 25.2% (at V_1 and V_2, respectively) lower than experimental values. Appling the correlation to the aluminum sphere covered by dry tissue underestimates the coefficients in 33.0% and 28.1% (at V_1 and V_2, respectively). Although the chosen correlation is appropriate for air flowing around a sphere, errors up to 30% are expected from empirical correlations estimating convective heat transfer coefficients (McAdams, 1954; Holman, 1992). McAdams correlation was obtained by a simplified linear regression to a big set of data, including spheres with different surface roughness and air flow under a large range of Reynolds numbers. It leads to differences even between these original data used to estimate the correlation and the predicted values.

Evaporative phenomena increased the heat transfer (resulting in an effective coefficient, h_{ef}) more than two-fold in all experimental setups with wet tissue compared with the same setup with dry tissue. Moreover, h and h_{ef} results in Table 1 show that increasing air velocity promotes significant coefficient increases ($p < 0.05$), as expected, while the RH did not affect h_{ef} significantly ($p > 0.05$) at either air velocity.

Table 1: h and h_{ef} values determined by experimental time-temperature data and by McAdams correlation for the two air velocities (with and without a cotton tissue) and three RH levels (only when the wet tissue covered the sphere). Results contain: average value ± standard deviation, and coefficient of variation in parentheses.

| Air velocity (m s⁻¹)	RH (%)	Uncovered sphere h (W m⁻² K⁻¹)		Sphere covered by the tissue h and h_{ef} (W m⁻² K⁻¹)		
				Dry tissue		Wet tissue
		McAdams correlation	Experimental	McAdams correlation	Experimental	Experimental
0.92 **(V_1)**	30	18.7	24.3 ± 2.1[a,A] (8.8)	18.9	28.2 ± 1.1[a,B] (4.0)	76.4 ± 5.3[a,C] (6.9)
	60					72.5 ± 3.5[a,C] (4.8)
	90					68.0 ± 4.1[a,C] (6.1)
1.42 **(V_2)**	30	24.0	32.1 ± 1.8[b,A] (3.0)	24.3	33.8 ± 2.5[b,A] (7.3)	97.8 ± 8.2[b,B] (8.3)
	60					93.1 ± 10.8[b,B] (11.7)
	90					91.3 ± 5.5[b,B] (6.0)

[a-b] Values in the same column with different lowercase letters indicate a significant difference ($p < 0.05$).
[A-C] Values in the same row with different capital letters indicate a significant difference ($p < 0.05$).

The difference in water vapor pressure between the wet tissue and the air (quantified by the RH values) is the driving force for mass transfer, promoting evaporation and increasing heat transfer and, consequently, resulting in $h_{ef} > h$ with the same experimental setup. Similar results were reported by Rainieri *et al*. (2009), who determined local heat transfer coefficients on an aluminum plate coated with a non-wetting material, on which dropwise condensation of water vapor was carried by a humid air stream. The results showed that, for a given air velocity, the heat transfer coefficient between air and the wet surface was up to six times higher than the values determined for the dry surface.

Chilling Times

Figure 2 presents time-temperature evolutions as an example of the six experimental replicates for the uncovered aluminum sphere (T_{Al}), covered by dry tissue, and covered by wet tissue at both air velocities. The dry tissue works as a thermal insulator, reducing heat transfer and increasing chilling time for both air velocities. On the other hand, a great reduction in cooling time was observed (e.g., more than three fold at RH = 60%), as a consequence of water evaporation on the sphere surface covered by the wet tissue. Evaporative cooling phenomena increased the heat transfer rates despite the thermal


(a)

(b)

(c)

(d)

(e)

(f)
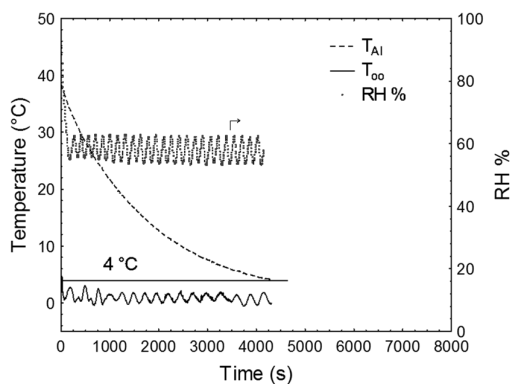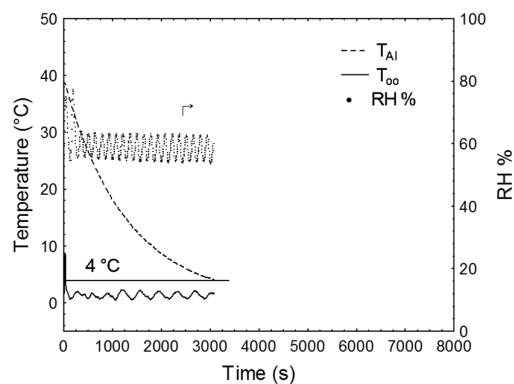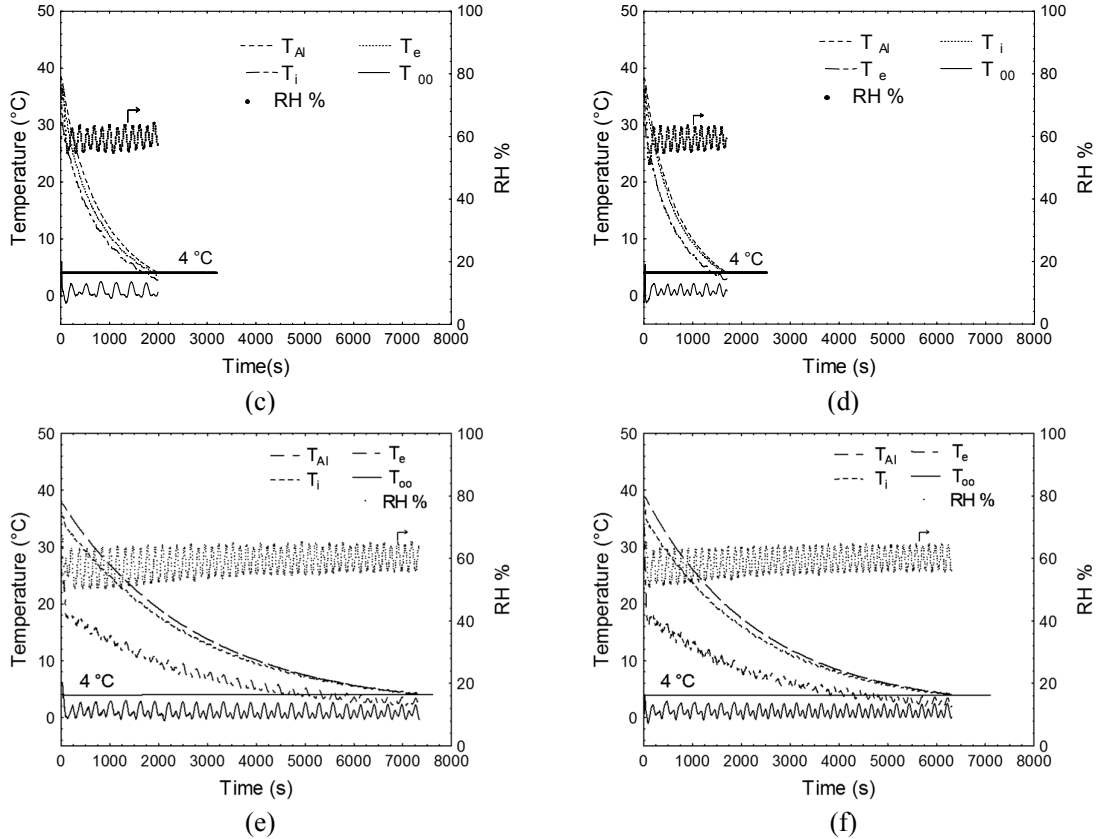
Figure 2: Time-temperature for the aluminum sphere (T_{Al}), cooling air (T_∞), and internal (T_i) and external (T_e) cotton tissue surfaces and time-RH evolution at two air velocities ($V_1 = 0.92$ m s^{-1} and $V_2 = 1.42$ m s^{-1}): (a) V_1 and (b) V_2- uncovered sphere; (c) V_1 and (d) V_2- sphere covered by wet tissue (RH = 60%); (e) V_1 and (f) V_2- sphere covered by dry tissue.

insulation associated with the wet tissue. This behavior was observed at all RH conditions and for both air velocities (data not shown).

Figure 3 illustrates the cooling time taking into account the core time-temperature evolution in the sphere covered with wet tissue at different RH and air velocities. As expected, the chilling time of the sphere covered with wet tissue decreased with lower RH and with the increase of air velocity inside of chamber. It shows a time increase close to 50% to reach 15 °C and a time increase over 70% to reach 4 °C (V1-90% compared to V2-30%).

Both experimental and adjusted time-water mass evolution of cotton tissue during evaporative cooling at different RH levels (30%, 60%, and 90%) and air velocities (V_1 and V_2) are presented in Figure 4. An initial water mass equal to 0.0338 kg (average values from experimental measurements) was assumed for all simulations. As illustrated in the figure, the

empirical Equation (Eq. (9)) was appropriate to represent the time-water mass evolution in cotton tissue during different experimental cooling conditions.
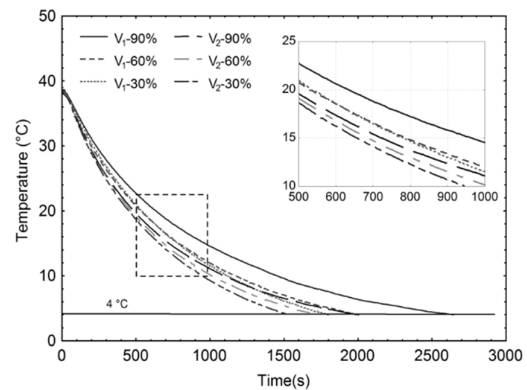
Figure 3: Cooling time of core time-temperature evolution in the sphere covered with wet cotton tissue for different RH and air velocities.
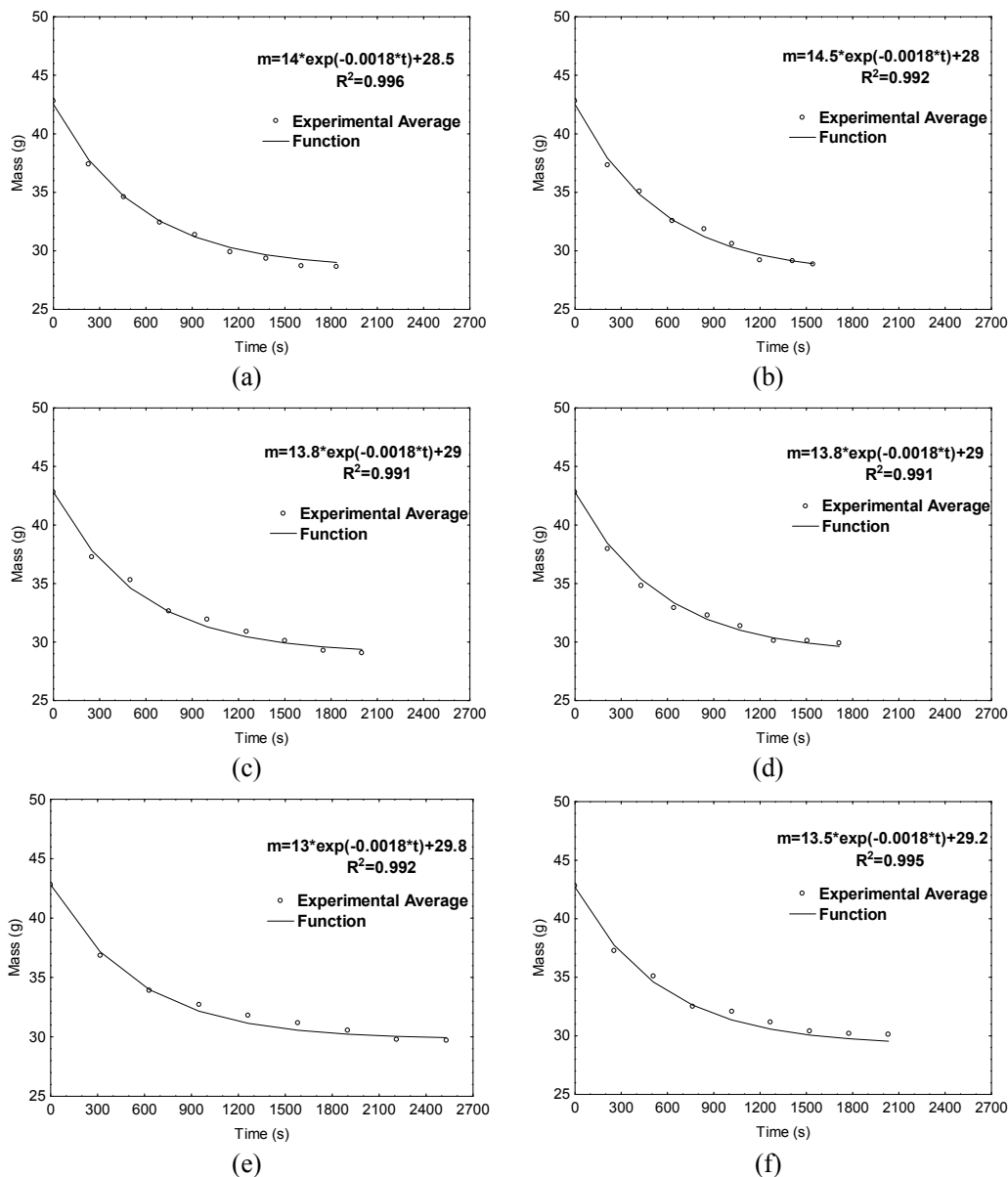
Figure 4: Experimental and adjusted time-water mass evolution of cotton tissue during cooling of the aluminum sphere covered by wet tissue in different conditions: (a) V_1-30%, (b) V_2-30%, (c) V_1-60%, (d) V_2-60%, (e) V_1-90%, (f) V_2-30%.

Table 2 summarizes experimental results comparing the influence of air velocity and RH on water loss (relative to the initial amount of water and determined by wet tissue weight reduction) and chilling time (time to reach T_{Al} = 4 °C). As expected, RH impacted water loss during cooling. Nevertheless, the largest difference was lower than 6% (37.6% and 42.1% of initial water content at V_2-90% and V_1-30%, respectively). The longest chilling time was at V_1 and RH = 90% (the worst condition, because of

the highest RH and lowest air velocity), requiring 65% more time to reach 4 °C in the sphere's core than the process performed at V_2 and RH = 30% (the best condition, because of the highest air velocity and lowest RH). Comparing experiments at the same air velocity, an RH increase from 30% to 90% extended the cooling time by 38% and 31%, at V_1 and V_2, respectively. These differences are meaningful and show the power of evaporative phenomena to enhance heat transfer in this kind of chilling process.

Table 2: Water loss by the wet tissue caused by the evaporative cooling, chilling time required to reach 4 °C, and correlation coefficients (R^2) obtained from regression of Eq. (9) to the water loss data. Data contain average value ± standard deviation, and coefficient of variation (in parentheses).

Air velocity (m s^{-1})	RH (%)	Percent of water loss by wet cotton (%)	Time for T_{Al} to reach 4 °C (s)	R^2 in Eq. (9) regression
0.92 (V_1)	30	42.1 ± 1.1[a] (2.7)	1841.7 ± 38.8[a] (2.1)	0.997
	60	41.1 ± 1.3[a,b] (3.1)	2015.0 ± 13.2[b] (0.6)	0.990
	90	38.9 ± 1.4[b,c] (3.5)	2541.7 ± 127.9[c] (5.0)	0.992
1.42 (V_2)	30	41.6 ± 0.6[a] (1.5)	1546.3 ± 25.6[d] (1.6)	0.992
	60	37.9 ± 1.9[c] (5.2)	1715.0 ± 9.4[e] (0.5)	0.994
	90	37.6 ± 0.8[c] (2.2)	2033.0 ± 79.7[b] (3.9)	0.994

[a-d] Values in the same column with different letters indicate a significant difference ($p < 0.05$).

CONCLUSIONS

The experimental approach proposed in this study allows assessing the effective heat transfer coefficient between a metal sphere covered with a moist cotton tissue and forced air. Under the investigated experimental conditions, an effective heat transfer coefficient approximately three-fold higher was found for the sphere covered with the moist cotton tissue. From a practical point of view, it is possible to increase heat transfer by spraying a solid surface (e.g., solid foods) with clean water, if it is tolerable. Moreover, the experimental results showed that it is possible to control product water loss by changing the velocity and RH of the cooling air. Many industrial processes, such as food cooling by air blast, can take advantage of these results. Moreover, this experimental approach, requiring only temperature measurements, can be tested in industrial plants, in which, in general, airflow and properties are expensive and impractical to be measured.

ACKNOWLEDGMENT

NOMENCLATURE

A_{Al}	Surface area of the aluminum sphere, (m^2)
A_e	Surface area of the aluminum sphere covered by the wet cotton tissue, (m^2)
CV	Coefficient of variation,
c_{Al}	Specific heat of the aluminum sphere, (J kg^{-1} K^{-1})
c_c	Specific heat of the wet cotton tissue, (J kg^{-1} K^{-1})
c_d	Specific heat of the dry cotton tissue, (J kg^{-1} K^{-1})
D_{Al}	Diameter of the aluminum sphere, (m)
D_e	Diameter of the aluminum sphere covered with cotton tissue, (m)
h	Convective heat transfer coefficient, (W m^{-2} K^{-1})
h_{ef}	Effective convective heat transfer coefficient (which considers the thermal and evaporative effect), (W m^{-2} K^{-1})
k_{Al}	Thermal conductivity of the aluminum sphere, (W m^{-1} K^{-1})
k_∞	Thermal conductivity of the gas (cooling air), (W m^{-1} K^{-1})
L	Characteristic dimension, (m)
m_{Al}	Mass of the aluminum sphere, (kg)
m_c	Mass of the wet cotton tissue, (kg)
m_d	Mass of the dry cotton tissue, (kg)
m_w	Mass of the water, (kg)
R_{conv}	Convective thermal resistance
R_{cot}	Conductive thermal resistance of cotton
R_{sph}	Conductive thermal resistance of the sphere
RH	Relative humidity
r_e	External radius of the cotton tissue, (m)
r_i	Internal radius of the cotton tissue, (m)
t	Time, (s)
t_0	Initial condition of time, (s)
T_{Al}	Sphere's core temperature, (°C)
$\bar{T}_c$	Average temperature in the cotton spherical shell, (°C)
$T_c(r)$	Temperature of the spherical shell as a radial function, (°C)
T_e	External temperature of the cotton surface, (°C)
T_i	Internal temperature of cotton, (°C)
T_o	Aluminum sphere temperature at time t_o, (°C)
T_∞	Cooling air temperature, (°C)
V_1	Air velocity 1 (0.92 m s^{-1}), (m s^{-1})
V_2	Air velocity 2 (1.42 m s^{-1}), (m s^{-1})

V_1-30%   Chilling process with air velocity 1 and
          RH= 30%

V_1-60%   Chilling process with air velocity 1 and
          RH= 60%

V_1-90%   Chilling process with air velocity 1 and
          RH = 90%

V_2-30%   Chilling process with air velocity 2 and
          RH = 30%

V_2-60%   Chilling process with air velocity 2 and
          RH = 60%

V_2-90%   Chilling process with air velocity 2 and
          RH = 90%

Greek Letters

v Kinematic viscosity of cooling air, $(m^2 s^{-1})$

ρ_{Al} Density of the aluminum sphere, $(kg\ m^{-3})$

ρ_{∞} Density of the gas (cooling air), $(kg\ m^{-3})$

REFERENCES

Amendola, M. and Teruel, B., Uso de um esquema implícito e de splines para a simulação numérica do processo de resfriamento de frutas esféricas. Rev. Bras. Eng. Agríc. Amb., 9, 78-82 (2005). (In Portuguese).

Becker, B. R. and Fricke, B. A., Heat transfer coefficients for forced-air cooling and freezing of selected foods. Int. J. Refrig., 27, 540-551 (2004).

Carciofi, B. A. M. and Laurindo, J. B., Water uptake by poultry carcasses during cooling by water immersion. Chem. Eng. Proc., 46, 444-450 (2007).

Carciofi, B. A. M. and Laurindo, J. B., Experimental results and modeling of poultry carcass cooling by water immersion. Ciênc. Tec. Ali., 30, 447-453 (2010).

Chuntranuluck, S., Wells, C. M. and Cleland, A. C., Prediction of chilling times of foods in situations where evaporative cooling is significant–Part 1. Model development. J. Food Eng., 37, 111-125 (1998).

Cuesta, F. J., Lamúa, M. and Alique, R., A new exact numerical series for the determination of the biot number: Application for the inverse estimation of the surface heat transfer coefficient in food processing. Int. J. Heat Mass Transf., 55, 4053-4062 (2012).

Dincer, I., New effective Nusselt-Reynolds correlations for food-cooling applications. J. Food Eng., 31, 59-67 (1997a).

Dincer, I., Heat Transfer in Food Cooling Applications. Taylor & Francis, Washington, DC (1997b).

Erdogdu, F., Sarkar, A. and Singh, R. P., Mathematical modeling of air-impingement cooling of finite slab shaped objects and effect of spatial variation of heat transfer coefficient. J. Food Eng., 71, 287-294 (2005).

Holman, J. P., Heat Transfer. McGraw-Hill, London, UK (1992).

Huezo, R., Smith, D. P., Northcutt, J. K. and Fletcher, D. L., Effect of immersion or dry air chilling on broiler carcass moisture retention and breast fillet functionality. J. Appl. Poult. Res., 16, 438-447 (2007).

Incropera, F. P. and Dewitt, D. P., Fundamentos de transferência de calor e de massa. LTC, Rio de Janeiro, Brazil (2002). (In Portuguese).

James, C., Vincent, C., Lima, T. I. and James, S. J., The primary chilling of poultry carcasses - a review. Int. J. Refrig., 29, 847-862 (2006).

Jeong, J. Y., Janardhanan, K. K., Booren, A. M., Harte, J. B. and Kang, I., Breast meat quality and consumer sensory properties of broiler carcasses chilled by water, air, or evaporative air. Poult. Sci., 90, 694-700 (2011).

Landfeld, A. and Houska, M., Prediction of heat and mass transfer during passage of the chicken through the chilling tunnel. J. Food Eng., 72,108-112 (2006).

Laurindo, J. B., Carciofi, B. A. M., Silva, R. R. and Hense, H., On-line monitoring of heat transfer coefficients in a stirred tank from the signatures of the resultant force on a submerged body. Int. J. Refrig., 33, 600-606 (2010a).

Laurindo, J. B., Carciofi, B. A. M., Silva, R. R., Dannenhauer, C. E. and Hense, H., Evaluation of the effects of water agitation by air injection and water recirculation on the heat transfer coefficients in immersion cooling. J. Food Eng., 96, 59-65 (2010b).

Lucas, T. and Raoult-Wack, A. L., Immersion chilling and freezing in aqueous refrigerating media: Review and future trends. Int. J. Refrig., 21, 419-429 (1998).

McAdams, W. H., Heat Transmission. McGraw-Hill, New York (1954).

Mekprayoon, R. and Tangduangdee, C., Influence of Nusselt Number on weight loss during chilling process. Proc. Eng., 32, 90-96 (2012).

Mielnik, M. B., Dainty, R. H., Lundby, F. and Mielnik, J., The Effect of evaporative air chilling and storage temperature on quality and shelf life of fresh chicken carcasses. Poult Sci., 78, 1065-1073 (1999).

Rainieri, S., Bozzoli, F. and Pagliarini, G., Effect of a hydrophobic coating on the local heat transfer coefficient in forced convection under wet conditions. Exp. Heat Transf., 22, 163-177 (2009).

Sun, D.-W. and Wang, L., Experimental investigation of performance of vacuum cooling for commercial large cooked meat joints. J. Food Eng., 61, 527-532 (2004).

Teruel, B., Cortez, L. and Neves Filho, L., Estudo comparativo do resfriamento de laranja valência com ar forçado e com água. Ciênc. Tec. Ali., 23, 174-178 (2003). (In Portuguese).

Trujillo, F. C. and Pham, Q. T., A Computational fluid dynamic model of the heat and moisture transfer during beef chilling. Int. J. Refrig., 29, 998-1009 (2006).

Verboven, P., Scheerlinck, N. and Nicolai, B. M., Surface heat transfer coefficients to stationary spherical particles in an experimental unit for hydrofluidisation freezing of individual foods. Int. J. Refrig., 26, 328-336 (2003).